Int. J. Heat Mass Transfer. Vol. 26, No. 6, pp. 833–840, 1983
Printed in Great Britain

0017-9310/83/060833-08 $03.00/0
Pergamon Press Ltd.

HEAT TRANSFER IN NUCLEATE POOL BOILING AT HIGH HEAT FLUX

A. M. BHAT
Mechanical Engineering Department, Regional Engineering College, Srinagar, Kashmir 190006, India

R. PRAKASH*
Mechanical and Industrial Engineering Department, University of Roorkee, Roorkee 247672, India

and

J. S. SAINI
Alternate Hydro Energy Centre, University of Roorkee, Roorkee 247672, India

(*Received* 22 *December* 1981 *and in final form* 20 *September* 1982)

Abstract—An analytical model for heat transfer in nucleate pool boiling at high heat flux, near the critical value, is proposed. It is hypothesized that the heat transfer in this region takes place mainly due to the heat conduction through the liquid macrolayer formed on the heating surface. The results of the analysis have been compared with some experimental results and the agreement is found to be reasonably good.

NOMENCLATURE

c, specific heat of liquid [J kg^{-1} K^{-1}];
D_d, bubble departure diameter [m];
f, bubble departure frequency [Hz];
F, frequency of vapour mass [Hz];
g, acceleration due to gravity [m s^{-2}];
h, heat transfer coefficient [W m^{-2} K^{-1}];
h_{fg}, latent heat of vaporization [J kg^{-1}];
k, thermal conductivity of liquid [W m^{-1} K^{-1}];
N/A, number of active sites per m^2;
q_w, wall heat flux [W m^{-2}];
q_c, critical heat flux [W m^{-2}];
q_{cond}, conduction heat flux [W m^{-2}];
q_{nuc}, nucleation heat flux [W m^{-2}];
t, time [s];
T, T_w, T_s, temperature, wall temperature, saturation temperature [K];
ΔT, wall superheat, $T_w - T_s$ [K].

Greek symbols

α, thermal diffusivity of liquid [m^2 s^{-1}];
β, coefficient of thermal expansion of liquid [K^{-1}];
δ, δ_0, macrolayer thickness, initial macrolayer thickness [m];
μ, coefficient of dynamic viscosity of liquid [N s m^{-2}];
ρ, ρ_v, density of liquid, density of vapour [kg m^{-3}].

INTRODUCTION

IT IS well known that a single nucleate boiling mechanism does not explain the heat transfer process in the whole regime of nucleate boiling. It has been shown [1–5] that the nucleate boiling regime can be divided into two main heat transfer regions, viz. (i) the region of isolated bubbles at low heat flux, and (ii) the region of interference at high heat flux. Gaertner [1], in his study on saturated pool boiling of water at atmospheric pressure on a horizontal copper surface, subdivided the region of interference into (a) the vapour mushroom region and, (b) the second transition region. This transition region lies within about 0.6 q_c and q_c.

The aim of the present work is to study the heat transfer mechanism in the high heat flux region between 0.6 q_c and q_c.

Macrolayer in nucleate boiling

According to Yu and Mesler [6], at high heat flux, a liquid film, called the 'macrolayer', exists beneath the growing vapour mass which is paramount in transferring heat (Fig. 1). Nucleation takes place at active sites on the heating surface and vapour stems are formed in the macrolayer which feed vapour to the overlying vapour mass [7]. Gaertner [1] made measurements of the thickness of this macrolayer and gave the following relationship for initial macrolayer thickness:

$$\delta_0 = 0.6 D_d \tag{1}$$

where D_d is the average diameter of vapour stems or average bubble departure diameter. The best fit into the experimental data of Gaertner and Westwater [8] on D_d in saturated pool boiling of water at atmospheric pressure has been found to be

$$D_d = 0.809 \times 10^5 q_w^{-1.4225}. \tag{2}$$

Iida and Kobayasi [9] also made measurements of the initial macrolayer thickness in the case of saturated pool boiling of water at atmospheric pressure over a horizontal surface. The best fit into their experimental

* To whom correspondence should be addressed.

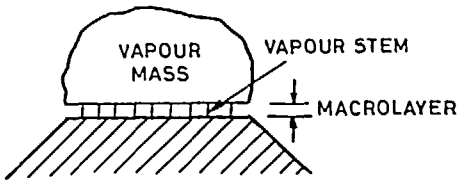

FIG. 1. Nucleate boiling at high heat flux.

data has been found to be

$$\delta_0 = 3.2296 \times 10^5 q_w^{-1.5148}. \quad (3)$$

Equations (1)–(3) show that the initial macrolayer thickness decreases with increase in heat flux.

The macrolayer, when initially formed, decreases in thickness due to consumption of its liquid in vapour generation during the growth period of the vapour mass [7].

ANALYSIS

Macrolayer of constant thickness

Assuming that (i) the macrolayer consists of a liquid without vapour stems, (ii) during the waiting period the macrolayer attains a uniform temperature, T_w, and (iii) at the end of the waiting period, when the formation of vapour mass is initiated, the temperature at the vapour–liquid interface on top of the macrolayer suddenly falls to T_s, while the temperature of the heating surface remains constant at T_w throughout the cycle, the conduction heat flux across the macrolayer of thickness δ may be found from the transient conduction equation

$$\alpha \frac{\partial^2 T}{\partial x^2} = \frac{\partial T}{\partial t}. \quad (4)$$

Based on the above assumptions, which may be stated mathematically as $T(x,0) = T_w$, $T(0,t) = T_w$ and $T(\delta,t) = T_s$, equation (4) may be solved using Laplace transformation, and the heat flux at the top surface of the macrolayer obtained as (Appendix 1)

$$q_{cond} = \frac{1}{(\pi\alpha t)^{1/2}} k\Delta T\left\{1+2\sum_{n=1}^{\infty} \exp\left[-\left(\frac{n\delta}{\alpha^{1/2}}\right)^2 \Big/ t\right]\right\}. \quad (5)$$

An expression for average conduction heat flux, averaged over time interval t_1, can be derived from equation (5) as (Appendix 2)

$$\bar{q}_{cond} = \frac{4k\Delta T}{t_1(\pi\alpha)^{1/2}}\left[\frac{t_1^{1/2}}{2} + \sum_{n=1}^{\infty} \times \left\{-(\pi M)^{1/2}\,\mathrm{erfc}\left[\left(\frac{M}{t_1}\right)^{1/2}\right] + t_1^{1/2}\exp\left(-\frac{M}{t_1}\right)\right\}\right] \quad (6)$$

where

$$M = (n\delta)^2/\alpha.$$

Assuming that the waiting period is very small compared to the cycle period, t_1, of the vapour mass, equation (6) will give conduction heat flux across the macrolayer of constant thickness, δ under the assumed conditions.

For the above analytical model, an expression for the temperature profile in the macrolayer may be obtained as (Appendix 3)

$$T = T_w - (T_w - T_s)\left\{\sum_{n=0}^{\infty} \mathrm{erfc}\left[\frac{\delta(2n+1)-y}{2(\alpha t)^{1/2}}\right] - \sum_{n=0}^{\infty} \mathrm{erfc}\left[\frac{\delta(2n+1)+y}{2(\alpha t)^{1/2}}\right]\right\}. \quad (7)$$

Macrolayer of varying thickness

If a constant vapour generation rate is considered during the growth period of the vapour mass and it is assumed that the thickness of the macrolayer decreases due to consumption of its liquid in vapour generation [7] and that the total heat flux, q_w, is dissipated due to latent heat transport [6], the rate of reduction in macrolayer thickness is given by

$$\frac{d\delta}{dt} = -\frac{q_w}{\rho h_{fg}}.$$

This gives

$$\delta = \delta_0 - \frac{q_w t}{\rho h_{fg}}. \quad (8)$$

If a linear temperature distribution is assumed in the macrolayer for the entire cycle period of the vapour mass, the temperature difference across the macrolayer being ΔT, the heat conduction rate through the macrolayer can be written as

$$q_{cond} = k\frac{\Delta T}{\delta}. \quad (9)$$

Using equations (8) and (9), the average value of conduction flux over a cycle period of $1/F$ is given by

$$\bar{q}_{cond} = \left(\frac{\rho h_{fg} k\Delta T F}{q_w}\right)\ln\left[\frac{\delta_0}{(\delta_0 - q_w)/(\rho h_{fg} F)}\right]. \quad (10)$$

Equation (10) gives the conduction heat flux across the macrolayer, when reduction in the macrolayer thickness during the growth period of vapour mass is considered and the temperature distribution in the macrolayer is linear.

Heat flow due to vapour formation at active sites

If the bubbles formed at the active sites on the heating surface leave the surface with average bubble departure diameter D_d and average frequency f, then the heat transfer as a result of bubble formation may be obtained as

$$q_{nuc} = \frac{\pi D_d^3}{6}\rho_v h_{fg} f \frac{N}{A}. \quad (11)$$

RESULTS AND DISCUSSION

The results of the analysis have been applied to saturated pool boiling of water at atmospheric pressure on a horizontal copper surface, in the heat flux region between $0.6q_c$ and q_c. Equations (1) and (2) and the following relations have been used:

$$q_w = 1.57 \times 10^5 \Delta T^{0.6}; \quad [1]$$

$$fD_d = 0.111 \text{ m s}^{-1}; \quad [5]$$

$$\frac{N}{A} = \frac{1}{\pi D_d^2}\left(\frac{h-h_{nc}}{h_{nuc}-h_{nc}}\right); \quad [10]$$

$$h_{nc} = 0.15[g\beta c(\rho k)^2/\mu]^{1/3}\Delta T^{1/3}; \quad [10]$$

$$h_{nuc} = \frac{2}{\pi^{1/2}}(\rho ck)^{1/2} f^{1/2}. \quad [10]$$

The results of equation (6) are plotted in Fig. 2 for a cycle period of 10 ms and for different wall superheats. The wall heat flux, q_w, is shown by a cross on the curve for each wall superheat; the macrolayer thickness at these points is such that the conduction heat flux equals the wall heat flux. These values of the macrolayer thickness are plotted in Fig. 3 for cycle periods of 10 and 60 ms. Experimental values of the initial macrolayer thickness given by equation (1) are also plotted in Fig. 3. It is seen that the predicted values are much less than the experimental ones and that while the experimental values decrease with an increase in heat flux, the predicted values follow the reverse trend.

The results of equation (7) are shown in Fig. 4. The instantaneous temperature profiles in the macrolayer show that the temperature distribution approaches steady state very fast. It is seen that for a 50 μm thick layer the temperature profile becomes linear in about 3 ms. For a 10 μm thick layer this period is about 0.5 ms while for a 100 μm thick layer it is about 8 ms. Therefore for cycle periods of the order of 100 ms, it may be reasonable to assume linear temperature distribution in the macrolayer and to use equation (10) to calculate the conduction heat flux through the macrolayer.

The results of equation (10) are plotted in Fig. 5 which shows conduction heat flux against frequency of vapour mass for different wall superheats. Figure 5 also shows the frequency of vapour mass at which conduction heat flux equals wall heat flux; this frequency of vapour mass has been calculated for different wall superheats and plotted in curve 1 of Fig. 6. This curve shows that the conduction heat flux equals the wall heat flux at critical value at a vapour mass frequency of 11.5 s^{-1}.

Considering vapour stems in the macrolayer as shown in Fig. 1, the average diameter of the vapour stems being D_d [1], and assuming that the whole of the liquid in the macrolayer is consumed in the formation of vapour mass during each cycle, the vapour mass frequency may be expressed as

$$F = \frac{q_w}{\rho\delta_0\left(1-\frac{\pi}{4}D_d^2\frac{N}{A}\right)h_{fg}}. \quad (12)$$

Curve 2 of Fig. 6 gives a plot of equation (12), which shows frequency of vapour mass against wall heat flux. Equation (12) gives vapour mass frequency of 14 s^{-1} corresponding to the critical heat flux.

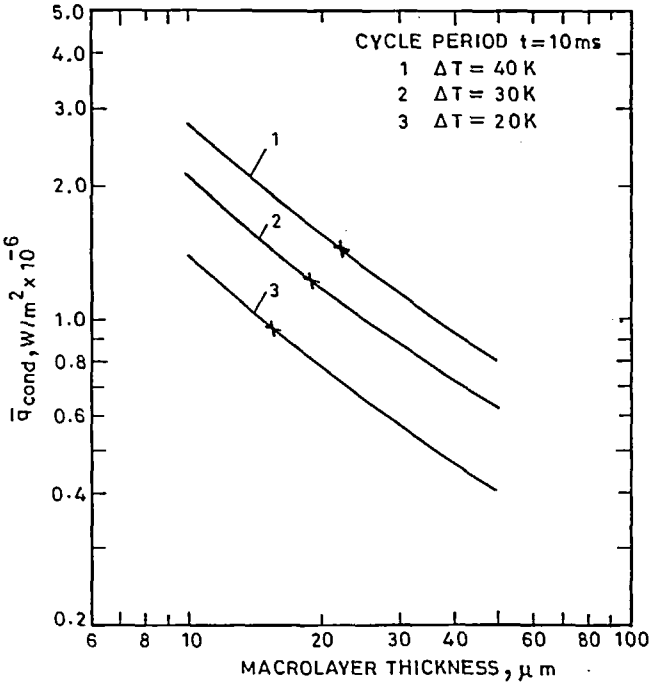

FIG. 2. Calculated transient conduction heat flux.

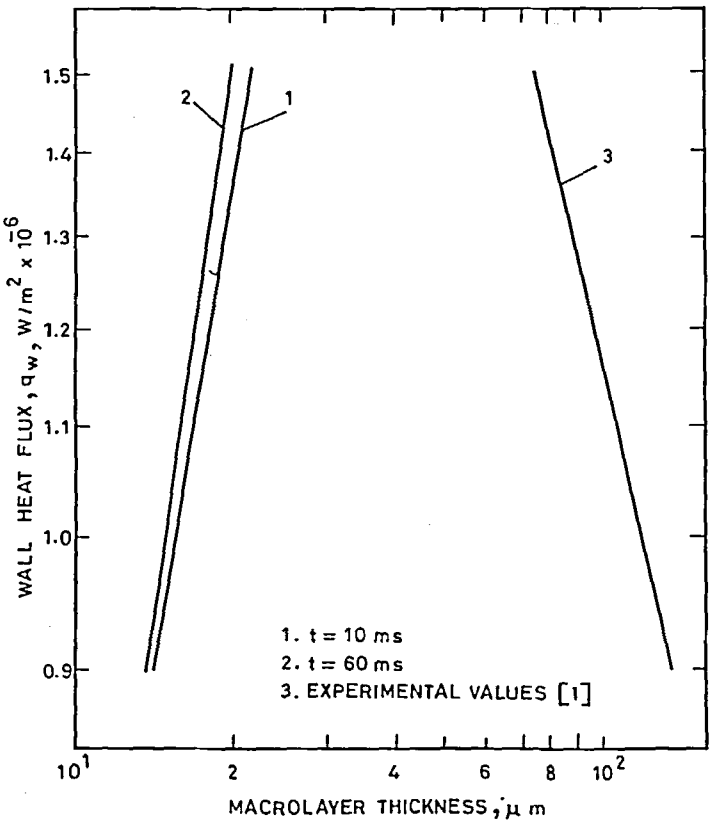

FIG. 3. Predicted macrolayer thickness in constant macrolayer thickness model compared with experimental values.

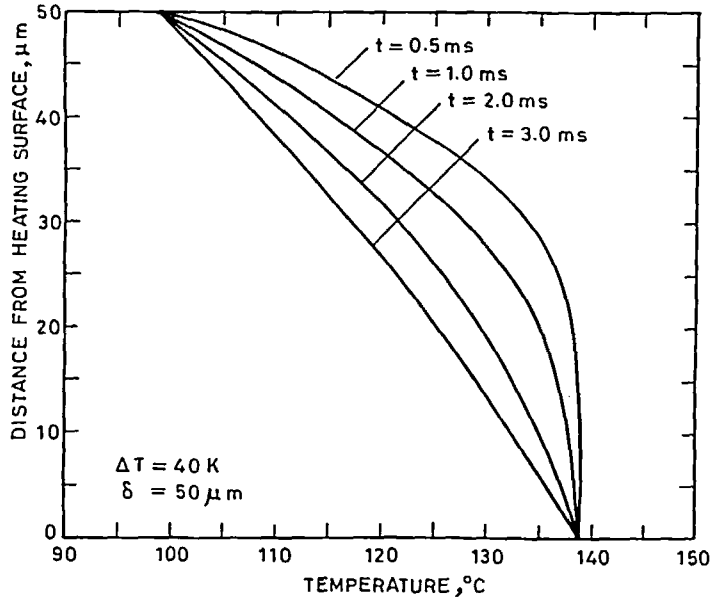

FIG. 4. Theoretical temperature profile in the macrolayer.

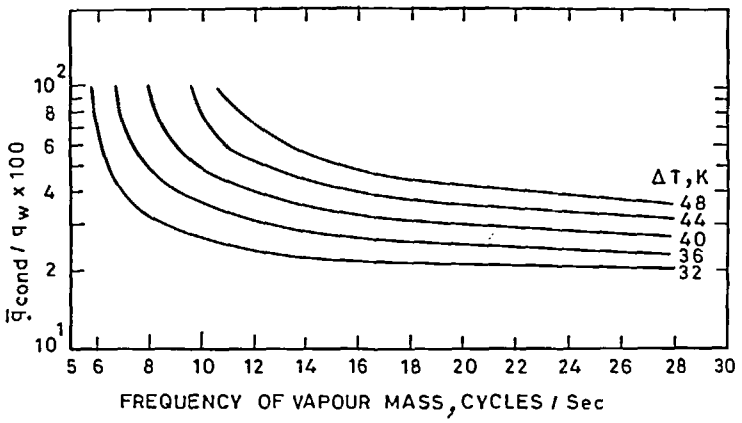

FIG. 5. Effect of frequency of vapour mass on conduction heat flux.

For the boiling conditions assumed in the above analysis, Iida and Kobayasi [9] reported the vapour mass frequencies between 10 and 25 s^{-1} in pool boiling experiments in the high heat flux region; Katto and Yokaya [7] reported a vapour mass frequency of 16 s^{-1} at a heat flux of 1.62×10^6 W m^{-2} and found that the frequency, which varied with heat flux, was nearly constant at any particular heat flux.

The results of equation (11) are shown in Fig. 7. It is seen that the contribution of q_{nuc} is insignificant in the entire high heat flux region, being less than 4.5% of the wall heat flux.

It is found from these results that direct vapour formation, due to bubble formation at active sites on the heating surface, does not account for much of the heat transfer in the high heat flux region. On the other hand, it is seen from Fig. 5 and Fig. 6 that, at appropriate values of the frequency of vapour mass, it is possible, in the varying macrolayer thickness model, for the macrolayer to conduct all the heat to its top from the heating surface. It thus seems plausible to presume that the bulk of the heat flows by conduction through, and consequent evaporation on top of, the macrolayer, while the macrolayer thickness decreases during the growth of the vapour mass due to consumption of its liquid. Reduction in the thickness of the macrolayer during growth of the vapour mass, is also supported by the results of equation (12) (curve 2 of Fig. 6) which gives vapour mass frequency, at the critical heat flux, very close to the experimental value as mentioned above.

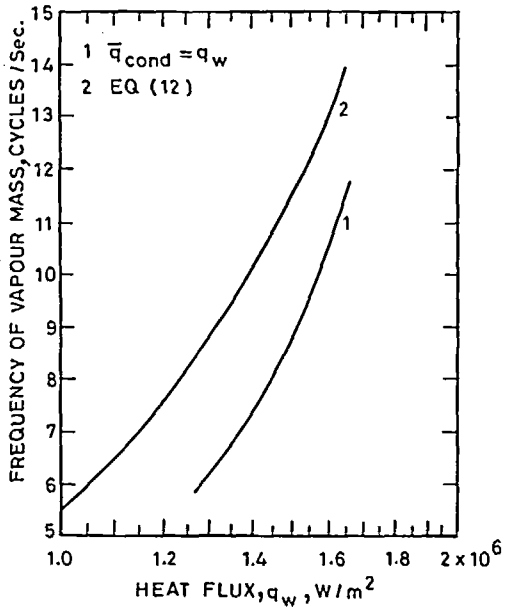

FIG. 6. Curve (1) theoretical frequency of vapour mass giving conduction heat flux equal to wall heat flux. Curve (2) theoretical frequency of vapour mass for complete consumption of liquid in the macrolayer.

This model is further supported by a recent investigation [6] which shows that at high heat flux, near the critical value, suppression of nucleate boiling takes place in the macrolayer beneath the vapour mass, when conduction through the macrolayer appears to be the only possible mode of heat transfer. It has been shown [6] that at high heat flux, in each cycle of vapour mass formation, nucleate boiling takes place first for a fraction of the cycle period, and then nucleate boiling gets suppressed until the vapour mass departs. Tolubinsky *et al.* [11], who studied heat transfer through thin liquid films, observed boiling suppression even at low and medium heat fluxes. At high heat fluxes, they observed suppression of nucleate boiling, followed by destruction of the liquid layer accompanied by dry patch formation.

CONCLUSIONS

Based on this work, the following mechanism of heat transfer in the high heat flux region is proposed:

(1) Heat conduction across the liquid macrolayer accounts for the major portion of heat transfer from the heated surface.

(2) In each cycle of vapour mass formation, nucleate boiling may get suppressed during part of the cycle when heat flows only by conduction across the macrolayer.

(3) The thickness of the macrolayer decreases during

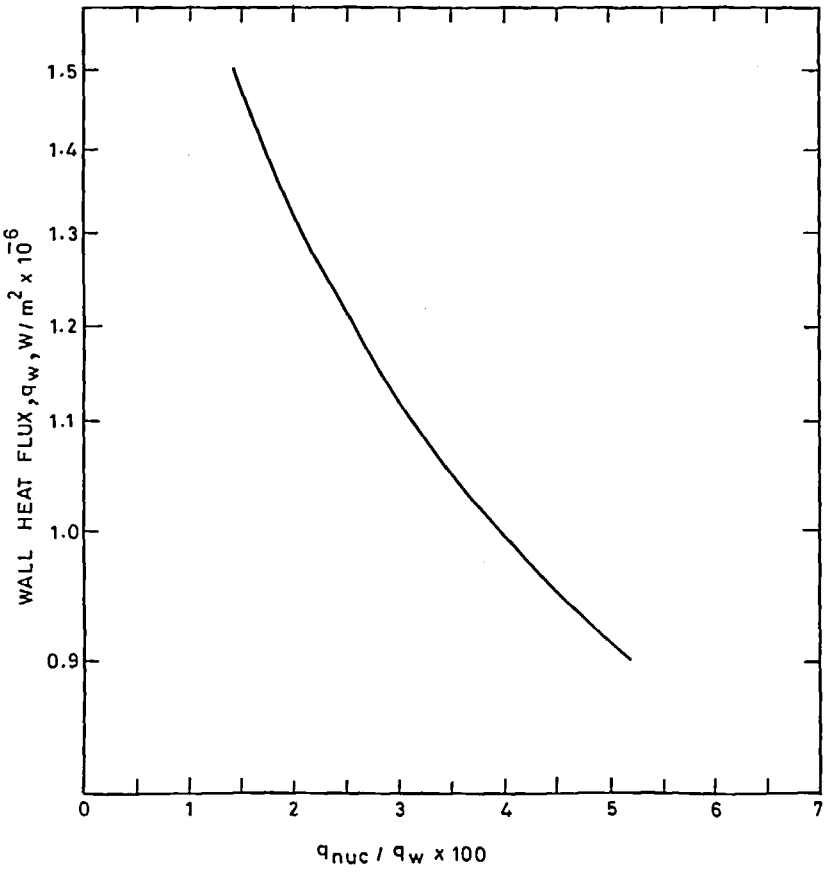

FIG. 7. q_{nuc} obtained from equation (11) as a fraction of q_w.

the cycle period due to consumption of its liquid in vapour generation.

REFERENCES

1. R. F. Gaertner, Photographic study of nucleate pool boiling on a horizontal surface, *Trans. Am. Soc. Mech. Engrs*, Series C, *J. Heat Transfer* **87**, 17–29 (1965).
2. R. Moissis and P. J. Berenson, On the hydrodynamic transitions in nucleate boiling, *Trans. Am. Soc. Mech. Engrs*, Series C, *J. Heat Transfer* **85**, 221–229 (1963).
3. N. Zuber, Nucleate boiling—the region of isolated bubbles and the similarity with natural convection, *Int. J. Heat Mass Transfer* **6**, 53–78 (1963).
4. D. B. Kirby and J. W. Westwater, Bubble and vapour behaviour on a heated horizontal plate during pool boiling near burnout, *Chem. Engng Prog. Symp. Ser.* **61** (57), 238–248 (1965).
5. K. Nishikawa and Y. Fujita, Correlations of nucleate boiling heat transfer based on bubble population density, *Int. J. Heat Mass Transfer* **20**, 233 (1977).
6. C.-L. Yu and R. B. Mesler, A study on nucleate boiling near the peak heat flux through measurement of transient surface temperature, *Int. J. Heat Mass Transfer* **20**, 827 (1977).
7. Y. Katto and S. Yokaya, Principal mechanism of boiling crisis in pool boiling, *Int. J. Heat Mass Transfer* **11**, 993 (1968).
8. R. F. Gaertner and J. W. Westwater, Population of active sites in nucleate boiling heat transfer, *Chem. Engng Prog. Symp. Ser.* **56**(30), 39 (1960).
9. Y. Iida and K. Kobayasi, Distribution of void fractions above a horizontal heating surface in pool boiling, *Bull. J.S.M.E.* **12**, 283 (1969).
10. K. Bier, D. Gorenflo, M. Salem and Y. Tanes, Pool boiling heat transfer and size of active nucleation centres for horizontal plates with different surface roughnesses, *Proc. 6th Int. Heat Transfer Conf.*, Canada, Vol. 1, p. 151 (1978).
11. V. I. Tolubinsky, V. A. Antonenko and Yu. N. Ostrovsky, Some heat transfer peculiarities in thin films of boiling liquid, *Proc. 6th Int. Heat Transfer Conf.*, Canada, Vol. 1, p. 175 (1978).
12. H. S. Carslaw and J. C. Jaeger, *Conduction of Heat in Solids* (2nd edn.). Oxford University Press, London (1959).
13. I. S. Gradshteyn and J. M. Ryzhik, *Tables of Integrals, Series Products*. Academic Press, New York (1965).
14. F. Oberhettinger and L. Badii, *Tables of Laplace Transforms*, Springer, Berlin (1973).

APPENDIX 1

Equation (4) and the initial and boundary conditions may be written as

$$\frac{\partial v}{\partial t} = \alpha \frac{\partial^2 U}{\partial x^2}, \tag{A1}$$

$$v(x,0) = 0, \tag{A2}$$

$$\left.\begin{aligned} v(0,t) &= 0, \\ v(\delta,t) &= 1, \end{aligned}\right\} \tag{A3}$$

where

$$v = \frac{T_w - T}{T_w - T_s}.$$

Taking Laplace transforms, we get

$$\frac{d^2\bar{v}}{dx^2} - \frac{p}{\alpha}\bar{v} = -\frac{1}{\alpha}v_0(x), \tag{A4}$$

$$\left.\begin{aligned}\bar{v} &= 0 \quad \text{at } x = 0, \quad t = 0\\ \bar{v} &= \frac{1}{p} \quad \text{at } x = \delta, \quad t > 0\end{aligned}\right\} \tag{A5}$$

where

$$v_0(x) = v(x) \quad \text{at } t = 0.$$

From equations (A2) and (A4), we get

$$\frac{d^2\bar{v}}{dx^2} - q^2\bar{v} = 0 \tag{A6}$$

where

$$q^2 = \frac{p}{\alpha}. \tag{A7}$$

The general solution of equation (A6) may be written as [12]

$$\bar{v} = A\,e^{qx} + B\,e^{-qx}. \tag{A8}$$

From equations (A5) and (A8), we get

$$\bar{v} = \left[\frac{e^{qx}}{p(e^{q\delta} - e^{-q\delta})} - \frac{e^{-qx}}{p(e^{q\delta} - e^{-q\delta})}\right]. \tag{A9}$$

Differentiating equation (A9) and rearranging the terms, we get

$$\frac{d\bar{v}}{dx} = \frac{q}{p}[e^{q(x-\delta)} + e^{-q(x+\delta)}](1 - e^{-2q\delta})^{-1}. \tag{A10}$$

By binomial series expansion, we may write

$$(1 - e^{-2q\delta})^{-1} = \sum_{n=0}^{\infty} e^{-2nq\delta}. \tag{A11}$$

From equations (A10) and (A11), we get

$$\frac{d\bar{v}}{dx} = \frac{q}{p}\sum_{n=0}^{\infty} e^{-q(\delta - x + 2n\delta)} + \frac{q}{p}\sum_{n=0}^{\infty} e^{-q(\delta + x + 2n\delta)}. \tag{A12}$$

Using equation (A7), we may write

$$\frac{q}{p}e^{-qx} = ap^{-1/2}\,e^{-ap^{1/2}x}$$

where

$$a = \alpha^{-1/2}.$$

From tables of inverse Laplace transforms [14],

$$L^{-1}[ap^{-1/2}\,e^{-ap^{1/2}x}] = a(\pi t)^{-1/2}\,e^{-(1/4)(ax)^2/t}.$$

Taking inverse Laplace transforms as above, we obtain from equation (A12)

$$\frac{dv}{dx} = a\sum_{n=0}^{\infty}(\pi t)^{-1/2}\,e^{-a^2[(2n+1)\delta - x]^2/(4t)} + a\sum_{n=0}^{\infty}(\pi t)^{-1/2}\,e^{-a^2[(2n+1)\delta + x]^2/(4t)}. \tag{A13}$$

Conduction heat flux at the top of the macrolayer may be obtained as

$$q_{cond} = q_{x=\delta} = -k\left.\frac{dT}{dx}\right|_{x=\delta}$$

or

$$q_{cond} = k(T_w - T_s)\left.\frac{dv}{dx}\right|_{x=\delta}. \tag{A14}$$

Using equation (A13) in equation (A14) and simplifying we get

$$q_{cond} = \frac{k\Delta T}{(\pi\alpha t)^{1/2}}\left[1 + 2\sum_{n=1}^{\infty} e^{-(n\delta a)^2/t}\right].$$

APPENDIX 2

Equation (5) may be written as

$$q_{cond} = \frac{k\Delta T}{(\pi\alpha)^{1/2}}\left\{\frac{1}{t^{1/2}} + 2\sum_{n=1}^{\infty}\left[\frac{e^{-(n\delta a)^2/t}}{t^{1/2}}\right]\right\} \tag{A15}$$

where

$$a = \alpha^{-1/2}$$

Average conduction heat flux, averaged over time interval t_1, may be obtained as

$$\bar{q}_{cond} = \frac{1}{t_1}\int_0^{t_1} q_{cond}\,dt$$

or

$$q_{cond} = \frac{1}{t_1}\frac{k\Delta T}{(\pi\alpha)^{1/2}}\left\{\int_0^{t_1}\frac{dt}{t^{1/2}} + 2\sum_{n=1}^{\infty}\int_0^{t_1}\left[\frac{e^{-(n\delta a)^2/t}}{t^{1/2}}\,dt\right]\right\}. \tag{A16}$$

The first integral in equation (A16) equals $2t_1^{1/2}$. The second integral may be written as

$$I = \int_{\infty}^{-1/t_1}\frac{e^{-MZ}}{Z^{3/2}}\,dZ$$

where

$$M = (n\delta a)^2$$

and

$$Z = \frac{1}{t}.$$

Integrating by parts, we obtain

$$I = -\left[-\frac{2e^{-MZ}}{Z^{1/2}} + 2M\int_{1/t_1}^{\infty}\frac{e^{-MZ}}{Z^{1/2}}\,dZ\right]$$

or

$$I = -\left\{-2\frac{e^{-MZ}}{Z^{1/2}} + 2M\left[\int_0^{\infty}\frac{e^{-MZ}}{Z^{1/2}}\,dZ - \int_0^{1/t_1}\frac{e^{-MZ}}{Z^{1/2}}\,dZ\right]\right\}. \tag{A17}$$

From tables of integrals [13]

$$\int_0^{\infty}\frac{e^{-MZ}}{Z^{1/2}}\,dZ = \left(\frac{\pi}{M}\right)^{1/2} \quad \text{for } Z > 0. \tag{A18}$$

Putting $MZ = u^2$, we obtain

$$\int_0^{1/t_1}\frac{e^{-MZ}}{Z^{1/2}}\,dZ = \frac{2}{M^{1/2}}\int_0^{(M/t_1)^{1/2}} e^{-u^2}\,du = \left(\frac{\pi}{M}\right)^{1/2}\left[\frac{2}{\pi^{1/2}}\int_0^{(M/t_1)^{1/2}} e^{-u^2}\,du\right] = \left(\frac{\pi}{M}\right)^{1/2}\text{erf}\,[(M/t_1)^{1/2}]. \tag{A19}$$

From equations (A16)–(A19), we obtain on simplification

$$\bar{q}_{\text{cond}} = \frac{4k\Delta T}{t_1(\pi x)^{1/2}}\left\{\frac{t_1^{1/2}}{2} + \sum_{n=1}^{\infty} t_1^{1/2}\, e^{-(M/t_1)} - (\pi M)^{1/2}\,\text{erfc}\,[(M/t_1)^{1/2}]\right\}.$$

APPENDIX 3

Equation (A9) may be rearranged as

$$\bar{v} = \frac{1}{p}\left(\frac{e^{qx}-e^{-qx}}{e^{q\delta}-e^{-q\delta}}\right)$$

or

$$\bar{v} = \frac{1}{p}[(e^{qx}-e^{-qx})\,e^{-q\delta}(1-e^{-2q\delta})^{-1}]. \quad \text{(A20)}$$

By binomial series expansion, we get

$$(1-e^{-2q\delta})^{-1} = \sum_{n=0}^{\infty} e^{-2nq\delta}. \quad \text{(A21)}$$

Using equation (A21) in equation (A20), and rearranging the terms, we obtain

$$\bar{v} = \frac{1}{p}\sum_{n=0}^{\infty} e^{-q[\delta(2n+1)-x]} - \frac{1}{p}\sum_{n=0}^{\infty} e^{-q[\delta(2n+1)+x]}. \quad \text{(A22)}$$

The terms in equation (A22) are of the form e^{-qx}/p, for which the inverse Laplace transform is obtained as [14]

$$L^{-1}\left[\frac{e^{-qx}}{p}\right] = \text{erfc}\left[\frac{x}{2(\alpha t)^{1/2}}\right].$$

So from equation (22) we obtain

$$v = L^{-1}(\bar{v}) = \sum_{n=0}^{\infty}\text{erfc}\left[\frac{\delta(2n+1)-x}{2(\alpha t)^{1/2}}\right] - \sum_{n=0}^{\infty}\text{erfc}\left[\frac{\delta(2n+1)+x}{2(\alpha t)^{1/2}}\right] \quad \text{(A23)}$$

where

$$v = \frac{T_w - T}{T_w - T_s}.$$

TRANSFERT THERMIQUE DANS L'EBULLITION NUCLEEE EN RESERVOIR A FLUX ELEVE

Résumé—On propose un modèle analytique pour le transfert thermique dans l'ébullition nucléée en réservoir à flux élevé près de la valeur critique. On suppose que le transfert thermique dans cette région est principalement dû à la conduction thermique à travers la microcouche de liquide formée sur la surface chaude. Les résultats de l'analyse sont comparés à quelques données expérimentales et l'accord est trouvé raisonnablement bon.

WÄRMEÜBERGANG BEIM BLASENSIEDEN IN FREIER KONVEKTION MIT HOHEN WÄRMESTRÖMEN

Zusammenfassung–Es wird ein analytisches Modell für das Blasensieden bei freier Konvektion mit hohen Wärmestromdichten in der Nähe des kritischen Wertes vorgeschlagen. Dabei wird von der Hypothese ausgegangen, daß der Wärmeübergang in diesem Bereich im wesentlichen durch die Wärmeleitung in der Flüssigkeits-Makro-Schicht bestimmt wird, die sich auf der Heizfläche ausbildet. Die Ergebnisse dieser analytischen Untersuchung wurden mit experimentellen Werten verglichen und verhältnismäßig gute Übereinstimmung festgestellt.

ТЕПЛОПЕРЕНОС ПРИ ПУЗЫРЬКОВОМ КИПЕНИИ В БОЛЬШОМ ОБЪЕМЕ ЖИДКОСТИ С ИНТЕНСИВНЫМ ПОДВОДОМ ТЕПЛА

Аннотация—Предложена аналитическая модель теплопереноса при пузырьковом кипении в большом объеме жидкости при высоком, почти критическом, тепловом потоке. Высказано предположение, что теплоперенос в этой области происходит в основном за счет теплопроводности через макрослой жидкости, образованный на поверхности нагрева. Проведено сравнение результатов анализа с некоторыми экспериментальными данными и получено довольно хорошее совпадение значений.